A New Active Control Process Based on Applying Critical Damping Theory in Two Vibration Modes

Javad ALAMATIAN
Civil Engineering Department, Mashhad Branch, Islamic Azad University, Mashhad, Iran, alamatian@mshdiau.ac.ir

Hamid DAVTALAB
Civil Engineering Department, Mashhad Branch, Islamic Azad University, Mashhad, Iran, hamiddavtalab@yahoo.com

Abstract: In this paper, a new active control procedure is presented using the developed critical damping concept. This strategy uses the well-known structural dynamics theories for improving the performance of critical damping (*CD*) method. In conventional *CD* algorithm, only the effect of first vibration mode has been incorporated to calculate the actuator force. The proposed method develops the critical damping concept so that the actuator force is formulated by considering the effects of the first and second vibration modes. This strategy improves the efficiency of the critical damping technique. Since the total damping matrix corresponding to the dynamic system should be semi positive definiteness, a novel approach is suggested here for determining the actuator and sensor locations. According to the proposed concepts, a new active control algorithm is obtained. Efficiency and stability of the proposed method is assessed by active control of vibrations of some shear buildings subjected to various dynamic loads. Results demonstrate considerable merit of the proposed active control algorithm compared to the common critical damping method.

Keywords: Smart Structure, Active Control, Critical Damping

1. INTRODUCTION

Vibration control and monitoring structural response are some of the most important subjects in dynamic analysis. In this regard, improving the seismic performance of structures and controlling their vibrations are very important so that smart structures are systems which can protect themselves against the external hazards such as earthquake and wind [1]. Such structures could modify their behaviors and adapt with dynamic effects [2]. In the other words, maintaining and improving the structural performance against the aforementioned excitations are important subjects known as structural control [1]. Several researches have been carried out on the field of structural control. These methods are categorized in three main groups including active, passive and semi-active techniques [3].

Passive control approach is a system in which the stiffness and damping of the structure are changed without requiring any external energy sources [4]. In these mechanisms, no external power source is required and control forces are generated in consequence of structural motion. Such controllers are utilized frequently due to the simplicity in their application and lack of external power requirements. However, the passive controllers are tuned only for a limited frequency range. Thus, in severe the seismic excitations, such controllers may increase the vibration amplitude especially near the resonance condition [1]. For this reason, active control methods, which possess high potential for using in wide range of frequencies, are introduced. Each active control procedure tries to reduce the vibrations based on a particular algorithm. In all strategies, minimization the vibrations amplitude in a shortest possible time is the main goal [2]. Active control systems always require an energy source for generating external forces, which affects the equilibrium equation of motion of the structure [1]. Actuator location and its applied force are important parameters in the performance of such systems. Improper algorithm of active control procedure may lead to instability and even collapse of structure. On the other hand, semi-active procedures are obtained by modifying the passive systems in combination with active control strategies [1].

Various active control algorithms have been introduced. Bayard et al. proposed the D-optimal principle in which the selected vibration's modes are transformed into a unitary form so that the suitable position of the piezoelectric element is obtained [5]. Kamada et al. modeled a four-story building using piezoelectric actuators [6]. Many researchers have also investigated the appropriate placement of piezoelectric actuators. Han and Lee employed genetic algorithm for finding the optimal locations of piezoelectric sensors and actuators [7]. Sadri et al.

used controllability Grammian criteria to locate the optimal placement of piezoelectric actuator [8]. To reduce the global noise level in a plate, Gao et al. used genetic algorithm for optimal placement of multi-actuators [9]. Based on the experimental results, Sethi and Song demonstrated the effectiveness of multi-modal active control of the smart frame structure using pole placement control [10]. Applying the Model Reference Adaptive Control into the Active Mass Dampers was studied numerically and experimentally for structures excited by the seismic effects [11]. Moreover, a time-delayed acceleration feedback controller was presented and applied to a cantilever beam for different controller gain–delay combinations [12]. A new performance index for active vibration control of three-dimensional structures was also suggested by Yanik and his co-workers [13]. The proposed performance index has been utilized for a six-story three-dimensional structure under several far-fault and near-fault earthquakes. On the other hand, an efficient computational approach was utilized for active control of nonlinear dynamic analysis of smart piezoelectric composite plates [14]. In another study, a fast-predictive control model was presented for large-scale structures subjected to earthquake ground motion [15]. The actuator force is obtained by solving one linear complimentarily problem and one transient analysis problem. In a recent research, an active-passive integrated vibration control method which has been used for the frequency domain analysis of truss structures demonstrates that this model could restrain the high-frequency vibrations and improve the characteristics of low-frequency vibrations [16].
In smart structures, appropriate performance of actuators and sensors depends on suitable placement of their locations as well as determining the actuators force. For this purpose, different algorithms such as Linear optimal control, discrete time-optimal control, pole assignment, nonlinear control, sliding mode control and using evolutionary algorithms like genetic algorithms and neural networks have been presented [1]. In these algorithms, the fundamental principles of structural dynamics are neglected. To overcome this defect, Alamatian and Rezaeepazhand, introduced a new algorithm based on critical damping theory [3]. In this method, known as *CD* procedure, single actuator is attached to the structure and modeled as an additional damper. The suitable locations of sensor and actuator are also determined based on modal shape vectors. On the other hand, they utilized this critical damping concept for controlling the frame's vibrations by introducing magnification factor [17]. In 2014, Karimpour et al. generalized the critical damping technique for the case of multi-actuators, which each actuator force is modeled as an equivalent viscous damper so that several vibration modes are damped critically [1]. Recently, linear actuator was utilized for active control based on real-time measurement of relative displacement [18].

From the applicability and economy point of views, structural control with single actuator i.e. *CD* technique, provides more suitable conditions in comparison with methods, use multi actuators. In the previous researches, the force of single actuator is calculated so that only the first vibration mode is critical [3]. In the other words, it is not possible to determine the actuator force by considering several vibration modes. Although the first mode has the most contribution in the dynamic response, incorporating the effects of higher modes could lead to a more efficient control procedure. This concept is evaluated here. For this purpose, the critical damping method is formulated by considering the effects of two vibration modes i.e. first and second, for determining the single actuator force. Therefore, a new method is proposed here for active structural control. Moreover, a new technique is presented here for determining the location of actuator and sensor by preserving the symmetry of equivalent damping matrix of controlled system.

2. CRITICAL DAMPING THEORY FOR ACTIVE CONTROL

If a structure is excited by dynamic hazards, the equilibrium equations of motion could be obtained by different methods such as Hamilton's principle [19]:

$$[\mathbf{M}]\{\ddot{\mathbf{D}}\}+[\mathbf{C}]\{\dot{\mathbf{D}}\}+[\mathbf{K}]\{\mathbf{D}\}=\{\mathbf{P}\} \qquad (1)$$

where $[\mathbf{M}]$, $[\mathbf{C}]$ and $[\mathbf{K}]$ are the structural mass, damping and stiffness matrices, respectively. Moreover, $\{\mathbf{P}\}$ and $\{\mathbf{D}\}$ are the external load and nodal displacement vectors, respectively. Control strategies try to reduce the dynamic response, obtained from Eq. (1). The critical damping (*CD*) concept is one of these techniques, which introduces a novel procedure for active control of structures [3]. In contrast to the common active control procedures, which use mathematical concepts, the critical damping technique utilizes structural dynamics theories. In this method, actuator is considered as an additional viscous damper and the actuator force is formulated so that the modal damping coefficients are critical. For the first time, this method was introduced by attaching single actuator and single sensor to the structure and the actuator force was formulated so that first modal damping becomes critical. Hence, the optimum actuator force is obtained at each time

instance. For this purpose, Eq. (1) is rewritten as follows [20]:

$$[\mathbf{M}]\{\ddot{\mathbf{D}}\}+[\mathbf{C}]\{\dot{\mathbf{D}}\}+[\mathbf{K}]\{\mathbf{D}\}+\{\mathbf{F}_a\}=\{\mathbf{P}\} \quad (2)$$

Here, $\{\mathbf{F}_a\}$ is actuator force vector. The vibrations will be damped as quickly as possible if the structural damping is critical. This concept is the main idea, which is used in the critical damping approach. By transforming Eq. (2) to the modal space, using following definition;

$$\{\mathbf{D}\}=[\mathbf{\Phi}]\{\mathbf{Z}\} \quad (3)$$

In Eq. (3), $\{\mathbf{Z}\}$ represents the modal displacement vector. By pre-multiplying Eq. (2) by the transpose of i^{th} modal shape vector i.e. $\{\boldsymbol{\varphi}_i\}$, equation of motion is written for i^{th} arbitrary mode. Assuming one actuator that is attached to the k^{th} degree of freedom, Eq. (3) is expressed as [3]:

$$M_i\ddot{Z}_i+C_i\dot{Z}_i+K_iZ_i+\varphi_{ki}F_a^k=\{\boldsymbol{\varphi}_i\}^T\{\mathbf{P}\} \quad (4)$$

where M_i, C_i and K_i are the mass, damping and stiffness of i^{th} vibration mode, respectively. Furthermore, F_a^k is the actuator force, applied to k^{th} degree of freedom and φ_{ki} denotes the k^{th} entry of i^{th} shape vector. Since the actuator is assumed as an additional damper, Eq. (4) could be re-arranged as follows:

$$M_i\ddot{Z}_i+\left(C_i+\frac{\varphi_{ki}F_a^k}{\dot{Z}_i}\right)\dot{Z}_i+K_iZ_i=\{\boldsymbol{\varphi}_i\}^T\{\mathbf{P}\} \quad (5)$$

The equivalent damping of i^{th} vibration mode, C_i^*, is defined as:

$$C_i^*=C_i+\frac{\varphi_{ki}F_a^k}{\dot{Z}_i} \quad (6)$$

The first mode has the most effect in dynamic response. Therefore, the equivalent damping of i^{th} vibration mode is assumed critical:

$$C_1^*=C_{cr}=2M_1\omega_1 \quad (7)$$

where M_1 and ω_1 are the modal mass and natural frequency corresponding to the first mode, respectively. On the other hand, choosing appropriate locations for actuator and sensor leads to optimal performance of active control algorithm. Based on previous studies, actuator should be attached to degree of freedom with largest value in the first modal shape vector [3]. Similarly, sensor should be attached to the degree of freedom with largest value in the first row of the inverse modal shape matrix [3]. Accordingly, $\dot{Z}_1$ could be approximated as follows [3]:

$$\dot{Z}_1\approx\varphi_{1L}^{-1}\dot{D}_L \quad (8)$$

where L is the location of sensor and φ_{1L}^{-1} denotes L^{th} entry in the first row of the inverse modal shape matrix. After determining the locations of sensor and actuator, based on the described procedure, the actuator force at each time instance is obtained [3]:

$$F_a^k=\frac{\varphi_{1L}^{-1}}{\varphi_{k1}}\left(2M_1\omega_1-C_1\right)\dot{D}_L \quad (9)$$

It should be noted that in common critical damping (*CD*) theory, the first vibration mode was only utilized for predicting the actuator force [3]. In this study, the first and second vibration modes are used to formulate the actuator force. This concept leads to a new active control method.

3. THE PROPOSED FORMULATION

In the common critical damping method, the effect of the first vibration mode is only considered. Although the first vibration mode is formed a significant portion of the dynamic response, applying the effects of higher modes could lead to a more accurate procedure. In the other words, the actuator force is formulated here by utilizing more than one vibration mode. This is a novel procedure, which is presented here. For applying such concept, it is assumed that one actuator is attached to the structure. Calculating the actuator force based on using the effect of first and second vibration modes is the final goal of this paper. First, Eq. (4) is rewritten for the first and second vibration modes:

$$\begin{cases}M_1\ddot{Z}_1+C_1\dot{Z}_1+K_1Z_1+\varphi_{k1}F_a^k=\{\boldsymbol{\varphi}_1\}^T\{\mathbf{P}\}\\ M_2\ddot{Z}_2+C_2\dot{Z}_2+K_2Z_2+\varphi_{k2}F_a^k=\{\boldsymbol{\varphi}_2\}^T\{\mathbf{P}\}\end{cases} \quad (10)$$

By modeling the actuator as a viscous damper, Eqs. (10) could be transformed as below:

$$\begin{cases}M_1\ddot{Z}_1+\left(C_1+\frac{\varphi_{k1}F_a^k}{\dot{Z}_1}\right)\dot{Z}_1+K_1Z_1=\{\boldsymbol{\varphi}_1\}^T\{\mathbf{P}\}\\ M_2\ddot{Z}_2+\left(C_2+\frac{\varphi_{k2}F_a^k}{\dot{Z}_2}\right)\dot{Z}_2+K_2Z_2=\{\boldsymbol{\varphi}_2\}^T\{\mathbf{P}\}\end{cases} \quad (11)$$

The first modal velocity, i.e. $\dot{Z}_1$ is determined from Eq. (8). Similar procedure could be performed for calculating the velocity of the second vibration mode i.e. $\dot{Z}_2$:

$$\dot{Z}_2\approx\varphi_{2L_2}^{-1}\dot{D}_{L_2} \quad (12)$$

In Eq. (12), L_2 is the location of the second sensor installation. For annihilating the vibrations caused by the 1^{th} and 2^{th} modes, the corresponding damping coefficients i.e. C_1^* and C_2^*, are assumed to be equal to critical values:

$$\begin{cases} C_1^* = C_{cr1} = 2M_1\omega_1 \\ C_2^* = C_{cr2} = 2M_2\omega_2 \end{cases} \quad (13)$$

By solving Eqs. (13), the actuator force is calculated so that the vibrations of the first and second modes damp critically;

$$\begin{cases} F_a^{k_1} = \dfrac{\varphi_{1L_1}^{-1}}{\varphi_{k_1}}\left(2M_1\omega_1 - C_1\right)\dot{D}_{L_1} \\ F_a^{k_2} = \dfrac{\varphi_{2L_2}^{-1}}{\varphi_{k_2}}\left(2M_2\omega_2 - C_2\right)\dot{D}_{L_2} \end{cases} \quad (14)$$

Here, $F_a^{k_1}$ and $F_a^{k_2}$ are corresponding actuator forces, which cause critical damping conditions in the first and second vibration modes, respectively. By superposing the effects of the first and second vibration modes, the actuator force is determined;

$$F_a^k = F_a^{k_1} + F_a^{k_2} = \frac{\varphi_{1L_1}^{-1}}{\varphi_{k_1}}\left(2M_1\omega_1 - C_1\right)\dot{D}_{L_1} + \frac{\varphi_{2L_2}^{-1}}{\varphi_{k_2}}\left(2M_2\omega_2 - C_2\right)\dot{D}_{L_2} \quad (15)$$

Eq. (15) shows that the actuator force is a function of velocities in the L_1^{th} and L_2^{th} degrees of freedom. On the other hand, Eq. (15) could be transformed into the matrix form:

$$F_a^k = \left[\bar{\mathbf{C}}\right]\left\{\dot{\mathbf{D}}\right\} \quad (16)$$

where, $\left[\bar{\mathbf{C}}\right]$ is the equivalent damping matrix due to attach the actuator to the main structure. It is clear that all entries of this matrix are zero except the elements corresponding to L_1^{th} and L_2^{th} columns in k^{th} row. Substituting Eq. (13) into Eq. (2), the equilibrium equation of motion is achieved:

$$\left[\mathbf{M}\right]\left\{\ddot{\mathbf{D}}\right\} + \left(\left[\mathbf{C}\right] + \left[\bar{\mathbf{C}}\right]\right)\left\{\dot{\mathbf{D}}\right\} + \left[\mathbf{K}\right]\left\{\mathbf{D}\right\} = \left\{\mathbf{P}\right\} \quad (17)$$

In this model, the actuator increases the equivalent damping of controlled structure. Moreover, $\left[\bar{\mathbf{C}}\right]$ is a non-symmetric matrix in its general form. This subject destroys the symmetry of total damping matrix and causes instability in step-by-step time integrations. According to the fundamental theories of structural dynamic, damping matrix should be positive semi-definite [21]. Therefore, it is necessary to preserve the symmetry of equivalent damping matrix of controlled system. This goal is accomplished if L_1 and L_2 are the same and equal to k. In the other words, the proposed method only requires one sensor, attached to the k^{th} degree of freedom i.e. both of sensor and actuator should be installed on the same degree of freedom. By applying this concept, $\left[\bar{\mathbf{C}}\right]$ represents a diagonal matrix in which k^{th} entry is as below:

$$\bar{C}(k,k) = \frac{\varphi_{1k}^{-1}}{\varphi_{k1}}\left(2M_1\omega_1 - C_1\right) + \frac{\varphi_{2k}^{-1}}{\varphi_{k2}}\left(2M_2\omega_2 - C_2\right) \quad (18)$$

So far, extensive researches have been conducted on finding the optimal locations of sensors and actuators [22-27]. In order to determine the location of sensor and actuator, the previously mentioned procedure, proposed by Alamatian and Rezaeepazhand, is followed [3]. According to this technique, the actuator is attached to a degree of freedom, which is corresponding to the largest value of the first row in modal shape matrix.

One could make a comparison between the proposed active control method, see Eq 15 and well-known critical damping theory [3]. Both of these active controllers utilize single actuator and one sensor to reduce vibrations. However, the actuator force in the proposed method is formulated by applying the effects of first and second vibration modes. In the well-known critical damping theory, the actuator and sensor could be attached to different degrees of freedom [3], however, both of actuator and sensor are installed on the same degree of freedom in the suggested active control procedure. In the next section, the efficiency of the proposed active control procedure will be verified through analyzing some numerical examples.

4. NUMERICAL EXAMPLES

To assess the ability of the proposed active control method, two numerical examples with various loading conditions are investigated. For this purpose, the suggested technique is combined with the Newmark time integration scheme. Then, the dynamic response of structure could be calculated at each time, using step-by-step procedure. A computer program developed by the authors carries out this process. The main steps of the proposed algorithm could be summarized as below:

1- Construct the mass, damping and stiffness matrices of the main structure, choose time step size Δt and let $n \to 0$

2- Determine the actuator location *k*, let sensor location $L \to k$

3- Calculate diagonal entries of $\left[\bar{\mathbf{C}}\right]$ through Eq. (18)

4- Let $\left[\mathbf{C}\right] \to \left[\mathbf{C}\right] + \left[\bar{\mathbf{C}}\right]$

5- Calculate displacement, velocity and acceleration vectors at the current step by using the Newmark scheme

6- Calculate actuator force utilizing Eq. (15)

7- Let $n \rightarrow n+1$

8- Terminate if the whole time domain is covered, otherwise go to 5

In the following, vibrations of some shear buildings are actively controlled by the proposed technique and results are compared with other methods such as critical damping (*CD*) scheme.

4.1. Six-story shear building

A six-story shear building according to Figure 1 is considered [28]. The mass and stiffness of each story has been shown in Figure 1. The damping matrix is constructed using the Rayleigh assumption with coefficient ratio 0.001. Time step for dynamic analysis is 0.05 sec. By solving an eigenvalue problem and determining the modal shape vectors, the locations of sensor and actuator could be obtained. The details of this procedure have been inserted in Table 1. Since the entry in the first modal shape vector corresponding to the 6th degree of freedom has the largest value, the actuator is attached to this degree of freedom. To preserve the symmetry of equivalent damping matrix of controlled system in the proposed scheme, the sensor is also installed on 6th degree of freedom. On the other hand, the largest value of the first row in the inverse of modal shape matrix occurs in 4th entry. Thus, the sensor is attached to 4th degree of freedom in critical damping method (*CD*). For the first study, this building is subjected to harmonic loads, shown in Figure 1. The time-history of 6th roof has been plotted in Figure 2. It is clear that the proposed method reduces the oscillations more efficient than the critical damping (*CD*) technique. For better comparison, maximum displacements of each story as well as maximum actuator force are reported in Table 2.

It is concluded that the proposed method has considerably decreased the maximum displacement of all stories compared with *CD* and control off procedures. Moreover, maximum required actuator force in the proposed method is less than the critical damping strategy.

In next analyses, harmonic loads are removed and the structure is excited by two kinds of ground acceleration i.e. far field and near field records. Figures 3 and 4 show *Manjil* (far field) and *Northridge* (near field) ground acceleration records, respectively. Using time steps as 0.005 sec and 0.01 sec for *Manjil* and *Northridge* earthquakes, respectively, the ability of the proposed method is investigated. The time-history displacement of 6th story for *Manjil* and *Northridge* earthquakes have been plotted in Figures 5 and 6, respectively. Evidently, the proposed method has better performance in comparison with the critical damping approach so that it could damp the vibrations quicker than *CD* approach. In addition, maximum displacement of different stories and maximum actuator force for *Manjil* and *Northridge* acceleration records have been inserted in Tables 3 and 4, respectively. It is concluded that proposed method causes more reduction in stories displacements compared with the critical damping technique. However, the maximum required actuator force of the proposed method is slightly greater than the *CD* case.

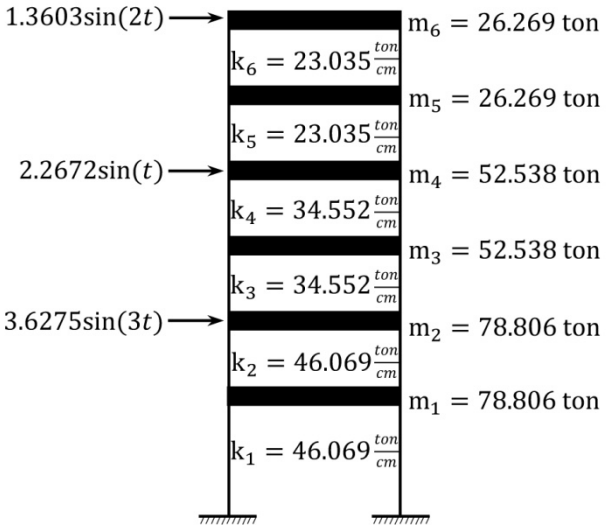

Figure 1. Six-story shear building

Table 1. The Actuator and Sensor Locations for six-story shear building

Degree of freedom	$\{\varphi_1^{inv}\}$	$\{\varphi_1\}$	Optimal control case	
			CD	*Proposed*
1	0.25756	0.12754	S4-A6	S6-A6
2	0.4893	0.24231		
3	0.4887	0.36302		
4	0.60777	0.45144		
5	0.35261	0.52383		
6	0.37782	0.56127		

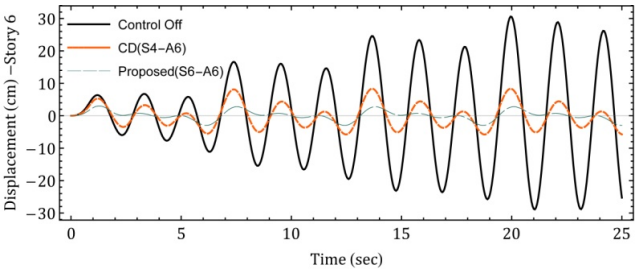

Figure 2 . Time history of roof displacement for six-story shear building subjected to the harmonic load

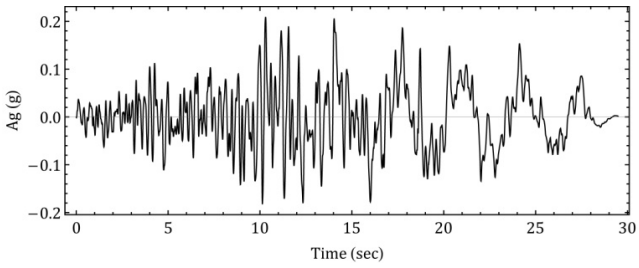

Figure 3. The Manjil base excitation

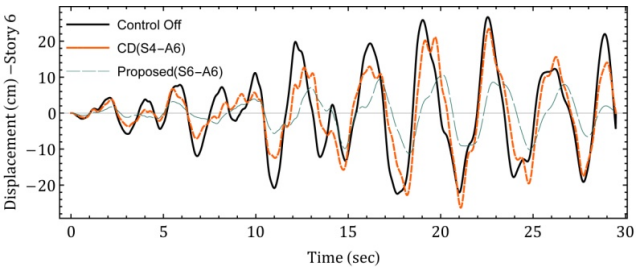

Figure 5. Time history of roof displacement for six-story shear building subjected to the Manjil base excitation

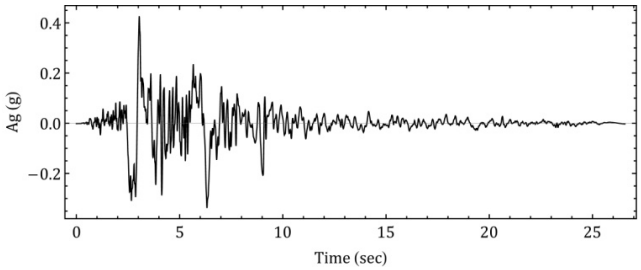

Figure 4. The Northridge base excitation

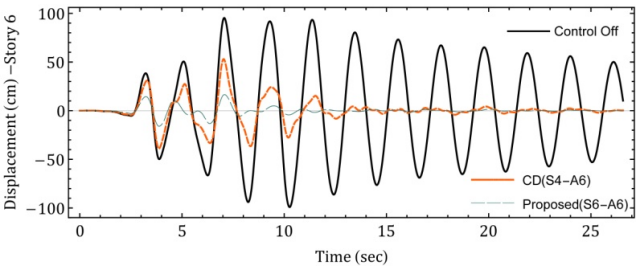

Figure 6. Time history of roof displacement for six-story shear building subjected to the Northridge base excitation

Table 2.Comparison of maximum response and maximum actuator force for six-story shear building subjected to the harmonic load

Story	Maximum displacement (cm)			Displacement reduction percentage (%)		Maximum actuator force (ton)	
	Control off	*CD*	*Proposed*	$\frac{Control\ \ off - Proposed}{Control\ \ off}$	$\frac{CD - Proposed}{CD}$	*CD*	*Proposed*
1	6.73	1.78	1.02	84.86	42.70	3.834	3.474
2	12.82	3.42	1.96	84.71	42.69		
3	19.44	5.12	2.40	87.67	53.13		
4	24.45	6.57	2.72	88.89	58.60		
5	28.40	7.61	2.83	90.02	62.81		
6	30.60	8.33	3.03	90.10	63.63		

Table 3. Comparison of maximum response and maximum actuator force for six-story shear building subjected to the Manjil base excitation

Story	Maximum displacement (cm)			Displacement reduction percentage (%)		Maximum actuator force (ton)	
	Control off	*CD*	*Proposed*	$\frac{Control\ \ off - Proposed}{Control\ \ off}$	$\frac{CD - Proposed}{CD}$	*CD*	*Proposed*
1	7.35	6.44	4.90	33.35	23.91	15.453	15.872
2	12.97	11.62	8.37	35.44	27.97		
3	17.05	16.61	10.95	35.79	34.08		
4	21.39	19.09	11.88	44.43	37.77		
5	24.88	22.58	11.55	53.56	48.85		
6	26.69	26.30	11.24	57.88	57.26		

Table 4. Comparison of maximum response and maximum actuator force for six-story shear building subjected to the Northridge base excitation

Story	Maximum displacement (cm)			Displacement reduction percentage (%)		Maximum actuator force (ton)	
	Control off	*CD*	*Proposed*	$\frac{Control\ \ off - Proposed}{Control\ \ off}$	$\frac{CD - Proposed}{CD}$	*CD*	*Proposed*
1	24.52	12.88	10.09	58.87	21.66	32.098	42.192
2	45.46	21.00	17.15	62.27	18.33		
3	64.35	25.09	21.89	65.98	12.75		
4	78.77	33.31	22.93	70.89	33.16		
5	91.87	45.49	18.63	79.72	59.05		
6	99.10	53.01	16.53	83.32	68.81		

4. 2. Ten-story shear building

Here, vibrations of a ten-story shear building shown in Figure 7 are actively controlled [29]. The damping matrix is constructed based on the Rayleigh principle with two factors i.e. the damping matrix is proportional to both mass and stiffness matrices. These two coefficients are calculated by assuming damping ratios of 5% for the first and third vibration modes. The fundamental period of vibration is 0.58 sec [28].

By solving an eigenvalue problem that its results have been presented in Table 5, locations of sensor and actuator could be determined. Since the largest value of the first modal shape vector occurs in the 10^{th} entry, the actuator (and hence sensor in the proposed method) will be attached to 10^{th} degree of freedom. Moreover, the sensor is installed on 9^{th} degree of freedom in the critical damping method.

For the first study, the structure is subjected to impact loads shown in Figure 8. Using time step as 0.005 sec, dynamic response is calculated. Figure 9 depicts the time-history of roof displacement. It is clear that the proposed active control method decreases the vibrations quicker than the *CD* approach. Furthermore, the maximum displacement of each story and maximum required actuator force are inserted in Table 6. Results prove that the suggested active control procedure could effectively reduce the maximum displacement in all degrees of freedom and demonstrates better performance compared to the *CD* method. However, the maximum required actuator force of the proposed technique is greater than the *CD* case.

In the next analyses, lateral loads are removed and the structure is excited by two ground acceleration records i.e. *Manjil* and *Northridge* earthquakes. The variation of roof displacement versus time has been plotted in Figure 10 for time step size 0.01sec if the *Manjil* earthquake ground acceleration record excites the building. Moreover, the maximum displacement of each story and maximum actuator force of this case are also inserted in Table 7. According to Table 7, it is clear that the displacement reduction of 8^{th}, 9^{th} and 10^{th} stories caused by the proposed method is greater than the *CD* technique; however, this improvement could not be seen in other stories. On the other hand, Figure 11 illustrates the time-history of roof displacement for the *Northridge* base excitation. The maximum displacement of each story and maximum actuator force are also inserted in Table 8.

It is observed that the proposed active control algorithm could efficiently reduce the maximum displacement in all stories. This reduction, of course, is greater than the critical damping method. However, the maximum required actuator force of the *CD* technique is less than the proposed scheme.

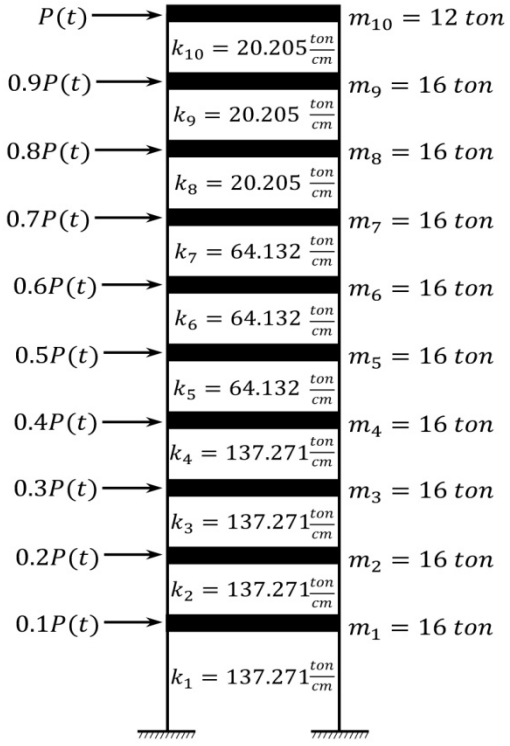

Figure 7. Ten-story shear building

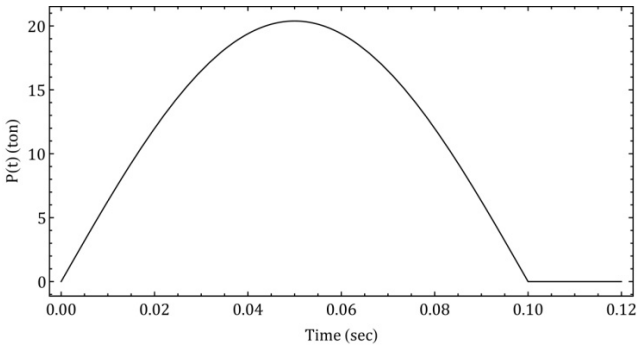

Figure 8. Time history of the impact load

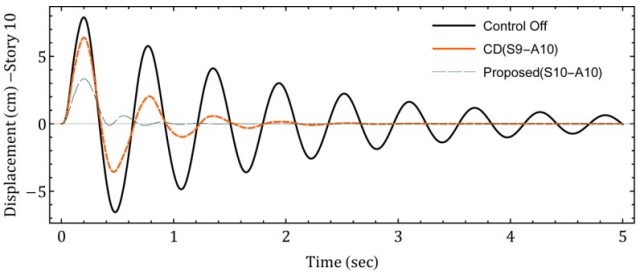

Figure 9. Time history of roof displacement for ten-story shear building subjected to the impact load

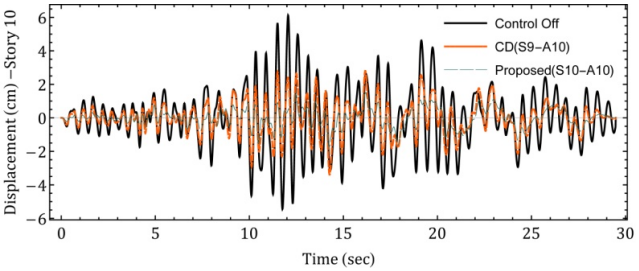

Figure 10. Time history of roof displacement for ten-story shear building subjected to the Manjil base excitation

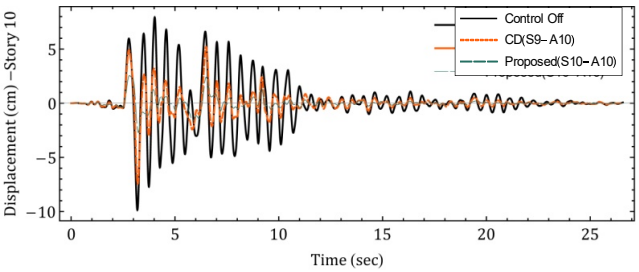

Figure 11. Time history of roof displacement for ten-story shear building subjected to the Northridge base excitation

Table 5. The actuator and Sensor Locations for ten-story shear building

Story	$\{\varphi_1^{inv}\}$	$\{\varphi_1\}$	Optimal control case	
			CD	*Proposed*
1	0.037102	0.034183	S9-A10	S10-A10
2	0.073688	0.067891		
3	0.10925	0.100656		
4	0.143293	0.132021		
5	0.211899	0.195229		
6	0.274199	0.252629		
7	0.328343	0.302513		
8	0.469189	0.432279		
9	0.565731	0.521226		
10	0.456638	0.560954		

Table 6. Comparison of maximum response and maximum actuator force for ten-story shear building subjected to the impact load

Story	Maximum displacement (cm)			Displacement reduction percentage (%)		Maximum actuator force (ton)	
	Control off	*CD*	*Proposed*	$\frac{Control\ \ off - Proposed}{Control\ \ off}$	$\frac{CD - Proposed}{CD}$	*CD*	*Proposed*
1	0.45	0.44	0.43	2.92	2.27	19.692	23.820
2	0.89	0.88	0.86	3.26	2.27		
3	1.32	1.30	1.26	4.73	3.08		
4	1.76	1.71	1.64	6.87	4.09		
5	2.66	2.54	2.35	11.66	7.48		
6	3.50	3.26	2.92	16.58	10.43		
7	4.22	3.85	3.28	22.18	14.81		
8	6.06	5.12	3.74	38.28	26.95		
9	7.27	5.85	3.45	52.44	41.03		
10	7.89	6.38	3.33	57.73	47.81		

Table 7. Comparison of maximum response and maximum actuator force for ten-story shear building subjected to the Manjil base excitation

Story	Maximum displacement (cm)			Displacement reduction percentage (%)		Maximum actuator force (ton)	
	Control off	*CD*	*Proposed*	$\frac{Control\ \ off - Proposed}{Control\ \ off}$	$\frac{CD - Proposed}{CD}$	*CD*	*Proposed*
1	0.39	0.23	0.31	20.99	-	10.665	16.627
2	0.75	0.44	0.59	20.45	-		
3	1.09	0.63	0.86	21.78	-		
4	1.43	0.79	1.08	23.92	-		
5	2.09	1.12	1.48	29.33	-		
6	2.70	1.45	1.76	34.91	-		
7	3.24	1.75	1.89	41.64	-		
8	4.68	2.6	1.88	59.79	27.69		
9	5.68	3.16	1.75	69.08	44.62		
10	6.12	3.39	1.73	71.71	48.97		

Table 8. Comparison of maximum response and maximum actuator force for ten-story shear building subjected to the Northridge base excitation

Story	Maximum displacement (cm)			Displacement reduction percentage (%)		Maximum actuator force (ton)	
	Control off	*CD*	*Proposed*	$\frac{Control\ \ off - Proposed}{Control\ \ off}$	$\frac{CD - Proposed}{CD}$	*CD*	*Proposed*
1	0.65	0.56	0.48	25.93	14.29	17.321	26.325
2	1.26	1.08	0.92	26.80	14.81		
3	1.84	1.56	1.32	27.96	15.38		
4	2.36	1.98	1.66	29.69	16.16		
5	3.39	2.78	2.25	33.70	19.06		
6	4.31	3.46	2.66	38.30	23.12		
7	5.13	4.02	2.88	43.83	28.36		
8	7.40	5.57	2.98	59.79	46.50		
9	9.09	6.82	2.75	69.73	59.68		
10	9.86	7.44	2.70	72.65	63.71		

5. CONCLUSION

In this paper, a novel approach was presented for improving the critical damping active control procedure. For this purpose, two vibration modes i.e. first and second were utilized to formulate the single actuator force. Here, the actuator force was assumed to produce fictitious viscous damping for dynamic system. As a result, the actuator force was formulated so that the first and second modes were damped critically. The proposed method utilizes single actuator and single sensor, which is suitable from applicability and economy point of view. Moreover, both actuator and sensor should be installed on same degree of freedom to guarantee the stability of active control procedure (positive semi-definite of equivalent damping matrix). To evaluate the efficiency of the proposed method in comparison with common critical damping strategy (*CD*), two shear structures including six-story and ten-story buildings were analyzed with various dynamic loads. Based on the numerical experiments, the proposed method has suitable ability to reduce the structural vibrations and preserve the stability of control process. Numerical results also demonstrate that the proposed method is not sensitive to the type of dynamic load so that it could efficiently decrease the maximum displacement of structures for various loads such as

harmonic force, impact load and base excitation (far field and near field earthquakes). In the other words, the proposed active method causes greater reduction in vibration's amplitude compared to the common critical damping (*CD*) technique. However, the maximum required actuator force of the proposed method is usually greater than the critical damping technique. This defect could be solved by increasing number of actuators. Thus, generalizing the proposed technique to the case of multi-actuators and multi-sensors could increase the efficiency of control process.

REFERENCES

[1] Karimpour, B., Keyhani, A., and Alamatian, J., New active control method based on using multiactuators and sensors considering uncertainty of parameters, *Advances in Civil Engineering*, 2014, pp. 1-10.

[2] Fisco, N., and Adeli, H., Smart structures: part I-active and semi-active control, *Scientia Iranica*, 18(3), 2011, pp. 275-284.

[3] Alamatian, J., and Rezaeepazhand, J., A simple approach for determination of actuator and sensor locations in smart structures subjected to the dynamic loads, *International Journal of Engineering-Transactions A: Basics*, 24(4), 2011, pp. 341-350.

[4] Korkmaz, S., A review of active structural control: challenges for engineering informatics, *Computers & Structures*, 89(23), 2011, pp. 2113-2132.

[5] Bayard, D.S., Hadaegh, F.Y., and Meldrum, D.R., Optimal experiment design for identification of large space structures, *Automatica*, 24(3), 1988, pp. 357-364.

[6] Kamada, T., Fujita, T., Hatayama, T., Arikabe, T., Murai, N., Aizawa, S., and Tohyama, K., Active vibration control of flexural-shear type frame structures with smart structures using piezoelectric actuators, *Smart materials and structures*, 7(4), 1998, pp. 479-487.

[7] Han, J.H., and Lee, I., Optimal placement of piezoelectric sensors and actuators for vibration control of a composite plate using genetic algorithms, *Smart Materials and Structures*, 8(2), 1999, pp. 257-266.

[8] Sadri, A., Wright, J., and Wynne, R., Modelling and optimal placement of piezoelectric actuators in isotropic plates using genetic algorithms, *Smart materials and structures*, 8(4), 1999, pp. 490-498.

[9] Gao, F., Shen, Y., and Li, L., The optimal design of piezoelectric actuators for plate vibroacoustic control using genetic algorithms with immune diversity, *Smart Materials and Structures*, 9(4), 2000, pp. 485-492.

[10] Sethi, V., and Song, G., Multimode vibration control of a smart model frame structure, *Smart materials and structures*, 15(2), 2006, pp. 473-485.

[11] Tu, J., Lin, X., Tu, B., Xu, J., and Tan, D., Simulation and experimental tests on active mass damper control system based on Model Reference Adaptive Control algorithm, *Journal of Sound and Vibration*, 333(20), 2014, pp. 4828-4842.

[12] An, F., Chen, W.D., and Shao, M.Q., Dynamic behavior of time-delayed acceleration feedback controller for active vibration control of flexible structures, *Journal of Sound and Vibration*, 333 (20), 2014, pp. 4789-4809.

[13] Yanik, A., Aldemir, U., and Bakioglu, M., A new active control performance index for vibration control of three-dimensional structures, *Engineering Structures*, 62-63, 2014, pp. 53-64.

[14] Phung-Van, P., Nguyen, L.B., Tran, L.V., Dinh, T.D., Thai, C.H., Bordas, S.P.A., Abdel-Wahab, M., and Nguyen-Xuan, H., An efficient computational approach for control of nonlinear transient responses of smart piezoelectric composite plates, *International Journal of Non-Linear Mechanics*, 76, 2015, pp. 190-202.

[15] Peng, H., Li, F., Zhang, S., and Chen, B., A novel fast model predictive control with actuator saturation for large-scale structures, *Computers and Structures*, 187, 2017, pp. 35-49.

[16] Zhang, Y., Zang, Y., Li, M., Wang, Y., and Li, W., Active-passive integrated vibration control for control moment gyros and its application to satellites, *Journal of Sound and Vibration*, 394, 2017, pp. 1-14.

[17] Alamatian, J., and Rezaeepazhand, J., Vibration suppression of down-scaled frames using a multi-criteria sensor/actuator placement algorithm, *International Journal of Modelling and Simulation*, 35(2), 2015, pp. 82-95.

[18] Vasile, O., Active vibration control for viscoelastic damping systems under the action of inertial forces, *Romanian Journal of Acoustics and Vibration*, 14 (1), 2017, pp. 54-58.

[19] Chopra, A.K., *Dynamics of structures*, Prentice Hall New Jersey, 1995.

[20] Preumont, A., *Vibration control of active structures: an introduction*, Springer Science & Business Media, 2011.

[21] Meirovitch, L., *Computational methods in structural dynamics*, Springer Science & Business Media, 1980.

[22] Arbel, A., Controllability measures and actuator placement in oscillatory systems, *International Journal of Control*, 33(3), 1981, pp. 565-574.

[23] Hać, A., and Liu, L., Sensor and actuator location in motion control of flexible structures, *Journal of sound and vibration*, 167(2), 1993, pp. 239-261.

[24] Devasia, S., Meressi, T., Paden, B., and Bayo, E., Piezoelectric actuator design for vibration suppression-placement and sizing, *Journal of Guidance, Control, and Dynamics*, 16(5), 1993, pp. 859-864.

[25] Dhingra, A., and Lee, B., Multiobjective design of actively controlled structures using a hybrid optimization method, *International journal for numerical methods in engineering*, 38(20), 1995, pp. 3383-3401.

[26] Kondoh, S., Yatomi, C., and Inoue, K., The positioning of sensors and actuators in the vibration control of flexible systems, *JSME international journal. Ser. 3, Vibration, control engineering, engineering for industry*, 33(2), 1990, pp. 145-152.

[27] Bruant, I., Coffignal, G., Lene, F., and Verge, M., A methodology for determination of piezoelectric actuator and sensor location on beam structures, *Journal of Sound and Vibration*, 243(5), 2001, pp. 861-882.

[28] Rostami, S., Shojaee, S., and Saffari, H., An explicit time integration method for structural dynamics using cubic B-spline polynomial functions, *Scientia Iranica*, 20(1), 2013, pp. 23-33.

[29] Rezaiee-Pajand, M., Sarafrazi, S.R., and Hashemian, M., Improving stability domains of the implicit higher order accuracy method, *International Journal for Numerical Methods in Engineering*, 88(9), 2011, pp. 880-896.